NOVEL SURFACE-ACOUSTIC WAVE TRANSDUCERS

R.C. WOODS

Department of Electronic & Electrical Engineering,
University of Sheffield, Mappin Street, Sheffield, S1 3JD, England.

The conventional means of launching a Surface Acoustic Wave on a piezoelectric substrate is by using an inter-digital transducer. A modified structure using multilayer deposition, but only a single critical photolithography stage, is proposed in this paper. The potential advantages of this structure include greater ease of manufacture and/or access to higher frequencies. Several variants of the basic principle are possible, and these are analysed using a simple equivalent circuit model. Experimental results for several fabricated devices, including apodised (weighted) transducers, are presented. These results show that the technique is a viable method of launching surface acoustic waves and that the flexibility of the concept should approach that of the conventional type of transducer, with much scope for future development of more advanced versions.

1. Introduction

Surface-acoustic wave (SAW) devices have found wide applications in areas requiring filters (e.g. television IF strips), delay lines (e.g. radar installations) or convolvers (e.g. communications equipment). In many cases the system design has been influenced by the smallest feature size which can be fabricated, which governs the maximum frequency of operation of the interdigital transducers (IDTs) used. A method of increasing the maximum usable frequency of an IDT (without increasing the photolithography requirements over those for conventional IDTs) would be useful because this would allow access to frequency bands previously outside the capability of SAW devices, as well as potentially making available increased bandwidth for information transfer. In addition, further applications, formerly precluded because of considerations of maximum frequency and photolithography linewidth, could be contemplated. Alternatively, cost reductions over devices made using existing techniques, achieved through relaxed photolithography requirements, would also be extremely advantageous.

Direct-writing by electron-beam-lithography (EBL) is a commonly-quoted route to high frequencies, but this technique is best suited to very low volume applications where low throughput in the fabrication process is acceptable; its consequent relatively

high cost prevents its use in all but the most specialised applications. A means of reaching high frequencies using, as far as possible, *conventional* microelectronics fabrication technology would have wide application, by extending the useful range of SAW components into L – band. At present, components with fundamental operating frequencies in excess of ~ 700 MHz are exceptional. For example, filters covering the cellular radio bands around 900 MHz are extremely difficult to manufacture with good yield if a reasonable specification is to be satisfied; most SAW oscillators operating at L – band do so using harmonics or frequency multiplication, both of which degrade their performance. The devices described in this paper have the potential of enabling efficient manufacture of miniaturised filtering and delay functions at these frequencies.

Conventional SAW devices employ IDTs having the structure shown in Fig. 1, or variations of it [1]. These launch (or receive) SAW in two opposing directions on the surface of a piezo-electric crystal. To launch a SAW with wavelength λ using a synchronics transducer, it is normally necessary to be able to fabricate reliably lines with a width $\lambda/4$, so that if the linewidth limit is W and the SAW velocity is v, the maximum synchronous frequency (or "centre-frequency", for a symmetrical bandpass filter) that can be used is $v/4W = f_0$ (assuming for simplicity the usual 50:50 mark:space ratio when fabricating fine metal lines). If very fine lines are used, then the resistivity of the "fingers" becomes an additional, important, cause of loss in the IDT. Variants on this basic transducer design are also used, such as the use of multiple electrodes within each acoustic wavelength or the use of harmonic operation, but in all cases the high-frequency limit in the device design is set by the photolithography linewidth achievable.

A type of transducer structure has recently been independently developed [2] in which the gaps between the "finger" electrodes are very narrow (and are defined by a layer of deposited anodic oxide). The linewidth requirement is only $\lambda/2$ for this "narrow gap" structure, so that the "narrow gap" transducer has the potential of increasing
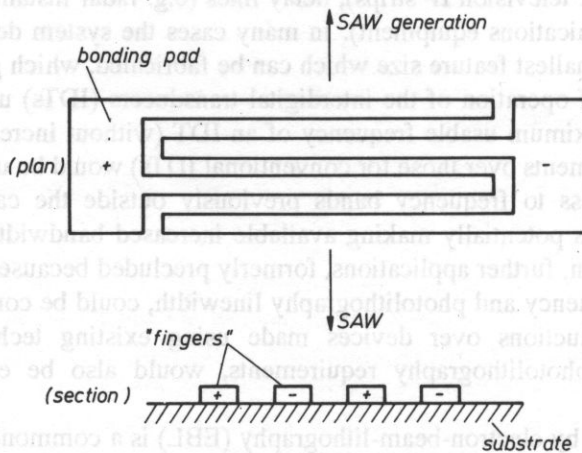

FIG. 1. Conventional SAW IDT. The electrodes are typically aluminium or gold thin films; the substrate is typically LiNbO₃, Quartz or GaAs .
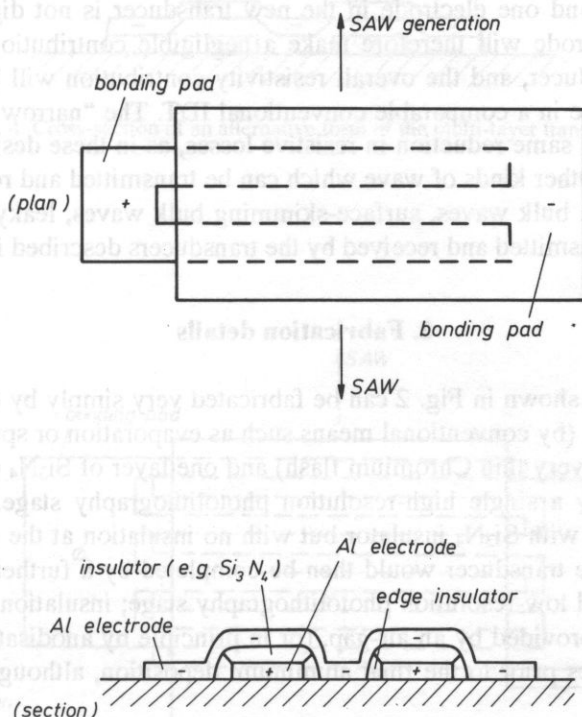
FIG. 2. One form of the multi-layer transducer described in this paper. If the buried electrode is made of aluminium, the edge insulation can be formed by anodisation, or alternatively an air-gap may be used.

the maximum usable frequency; the maximum attainable centre-frequency is $v/2W = 2f_0$.

The transducers described in this paper have the basic construction illustrated in Fig. 2; for this type of structure the required standard of photolithography is lower than for the conventional IDT or the "narrow gap" transducer [2] (i.e. the achievable smallest linewidth can be greater) because in the present devices "bridging" shorts between adjacent "fingers" do not substantially affect performance, whereas in the conventional device a "bridging" short between adjacent "fingers" immediately destroys the RF electric field which must be set up by the IDT in order for it to function. (A "bridging" short in a "narrow gap" transducer [2] may isolate part of the affected "finger(s)", depending on the mask design, thus giving less immunity from the effects of "bridging" shorts compared to the present structure.) If the linewidth achievable with this relaxed constraint is W', where $W' < W$, then the maximum attainable sampling frequency (or centre-frequency) is $v/2W'$ which is greater than twice f_0.

The "filling factor" of the electrodes contacting the crystal surface for the new type of transducer is different from that of the conventional IDT, and this may modify the minimum obtainable insertion loss. A further difference is that the transducer "fingers" are twice the width of those in the conventional IDT with the same bandwidth and

centre-frequency, and one electrode in the new transducer is not digitated at all; the non-digitated electrode will therefore make a negligible contribution to the resistive losses in the transducer, and the overall resistivity contribution will be approximately one quarter of those in a comparable conventional IDT. The "narrow gap" transducers [2] do not offer the same reduction in resistive losses, as in these designs *both* electrodes are digitated. Other kinds of wave which can be transmitted and received by a conventional IDT (e.g. bulk waves, surface-skimming bulk waves, leaky SAW [3] could, in principle, be transmitted and received by the transducers described in this paper.

2. Fabrication details

The transducer shown in Fig. 2 can be fabricated very simply by deposition of one layer of aluminium (by conventional means such as evaporation or sputtering, and usually preceded by a very thin Chromium flash) and one layer of Si_3N_4 (by plasma deposition) followed by a single high-resolution photolithography stage. This leaves the electrodes covered with Si_3N_4 insulator but with no insulation at the sides of the electrodes (Fig. 3). The transducer would then be completed by a further aluminium evaporation and a final low-resolution photolithography stage; insulation between the two electrodes can be provided by an air-gap, (or in principle by anodisation of the aluminium "finger" edges prior to the final aluminium deposition, although in practice this
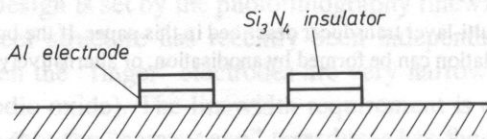

FIG. 3. Cross-section of the device water at an intermediate processing stage during fabrication of the structure shown in Fig. 2.

was found not to be necessary for the designs used in this work). It is an essential feature of the design that only *one* of the photolithography stages is highly critical, and precise alignment between the two stages is not important: the lithography for the digitated electrode and its insulation is "self-aligning".

An alternative structure, shown in Fig. 4, has also been investigated. In this case the initial (high-resolution) photolithography stage is performed only on the first aluminium layer, and the Si_3N_4 insulator and capping aluminium layer only need low-resolution processing; no anodising or other extra insulation is needed for this structure. It is expected that this construction would give increased insertion loss (see section 3).

A possible further variant is shown in Fig. 5, which shows a novel approach to the problem of designing a low-loss unidirectional transducer (UDT). Here the linewidth requirement is $\lambda/3$ (compared with $\lambda/6$ for a conventional UDT) and the design of the electrodes and crossovers is simplified over the conventional case. This type of UDT is the subject of future work.
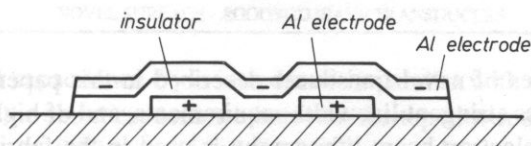
FIG. 4. Cross-section of an alternative form of the multi-layer transducer.
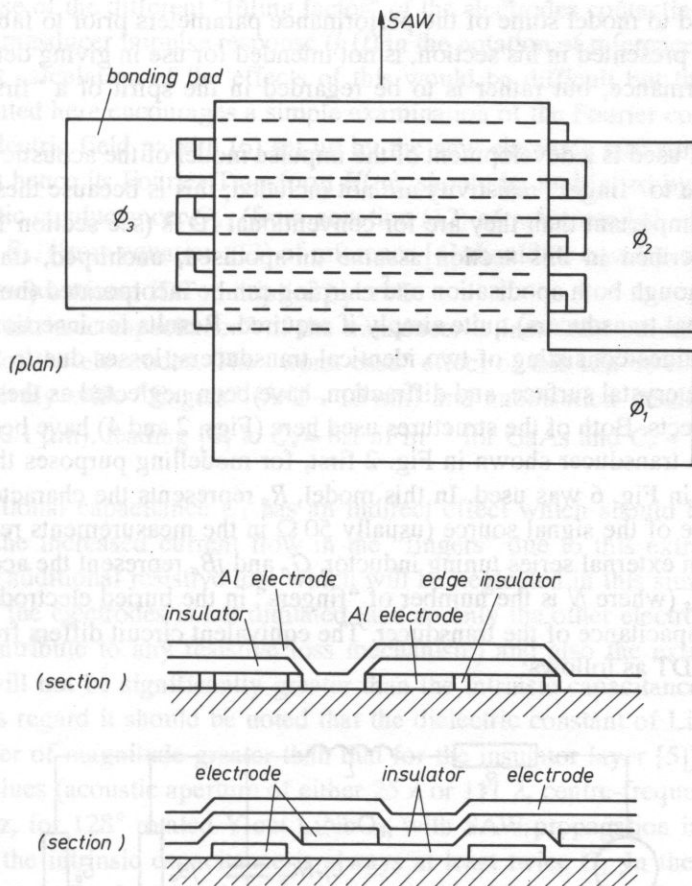

FIG. 5. A novel multi-layer approach to three-phase low-loss UDT design. The electrodes ϕ_1, ϕ_2 and ϕ_3 are driven using a 60° phase shifting circuit. (For simplicity the overlay insulators are not shown on the plan view). Several variants are possible depending on whether the structure is based on Fig. 2 or on Fig. 4 (see the two sectional views).

[155]

For all of the types of novel transducer described in this paper, the advantages of lower cost through less stringent linewidth requirements, and of higher frequency capability, still remain if electron-beam-lithography is used in the fabrication process, and in fact are obviously independent of the lithography technology used.

3. Simple model of transducers

An equivalent circuit model of the transducers described here has been developed for the purpose of quantifying some of the most important fundamental properties of the devices and to model some of the performance parameters prior to fabrication; this simple model, presented in his section, is not intended for use in giving detailed predictions of performance, but rather is to be regarded in the spirit of a "first order" approach.

The model used is a development of the impulse model of the acoustic conductance [4]. Losses due to "finger" resistivity are not included; this is because these losses will be much less important than they are for conventional IDTs (see section 1). All the simulations described in this section assume un-apodised, unchirped, transducers for simplicity, although both apodisation and chirping can be incorporated (both in the model and in actual transducers) quite simply if required. Results for insertion loss are given for delay lines consisting of two identical transducers; losses due to SAW attenuation along the crystal surface, and diffraction, have been neglected as these will usually be small effects. Both of the structures used here (Figs. 2 and 4) have been modelled.

Taking the transducer shown in Fig. 2 first, for modelling purposes the equivalent circuit shown in Fig. 6 was used. In this model, R_s represents the characteristic (internal) impedance of the signal source (usually 50 Ω in the measurements reported here), L represents an external series tuning inductor, G_a and jB_a represent the acoustic admittance, and NC_s (where N is the number of "fingers" in the buried electrode) represents the intrinsic capacitance of the transducer. The equivalent circuit differs from that for a conventional IDT as follows:
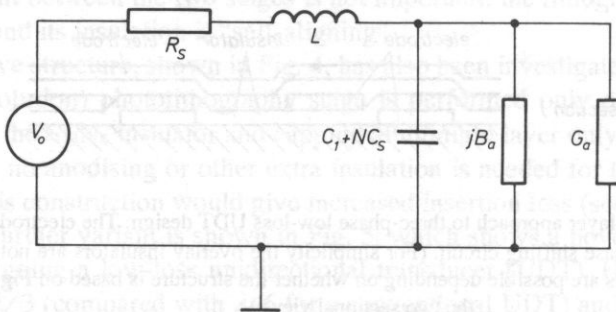

FIG. 6. The equivalent circuit used in this work to model the transducer shown in Fig. 2 (modified from reference [4]).

i. An additional capacitance C_1 is introduced in parallel with the acoustic admittance. This represents the shunt capacitance between the top electrode and the buried electrodes separated by a thickness, d, of insulator. Its value was estimated using the conventional "parallel plate" formula:

$$C_1 = \frac{\varepsilon_r \varepsilon_0 a N \lambda}{2d} \quad (+ \text{stray capacitance if necessary}) \tag{1}$$

where a is the transducer aperture (in metres), and ε_r is the relative permittivity of the insulator (taken to be 4.2 for Si_3N_4 [5]).

ii. Because of the different "filling factor" of the electrodes contacting the substrate surface, the transducer impulse response ($h(t)$ in the notation of reference [4]) is changed. An exact calculation of the effects of this would be difficult but the spirit of the model presented here encourages a simple examination of the Fourier components present in the electric field pattern [6] set up by the new electrode structure; this implies that $h(t)$, and hence its Fourier Transform $H(\omega)$, should be multiplied by $(\pi\sqrt{2})/4$, and so the acoustic conductance, G_a, (from equation (12) of reference [4] and the acoustic susceptance, B_a, (from equation (13) of reference [4] should be equal to their respective values for a conventional IDT multiplied by $\pi^2/8$.

iii. The "intrinsic capacitance" of the transducer is increased because of the large contact area of the electrodes. The "worst case" effect of this can be estimated by assuming relatively wide "fingers" ($\lambda/2 \sim 10\,\mu m$) and anodisation insulation which is very thin ($\sim 0.1\,\mu m$), leading [6] to $C_s = 6.1\,nFm^{-1}$ for GaAs and $C_s = 1.8\,nFm^{-1}$ for LiNbO$_3$.

The additional capacitance C_1 has an indirect effect which should be considered. Because of the increased current flow in the "fingers" due to this extra capacitance, there will be additional resistive loss which will be neglected in this simple model because one of the electrodes is not digitated (and so only the other electrode can be expected to contribute to any resistive loss mechanism) and also the extra capacitance introduced will not be significantly greater than the intrinsic capacitance of the transducer (in this regard it should be noted that the dielectric constant of LiNbO$_3$ is more than one order of magnitude greater than that for the insulator layer [5]). For realistic parameter values (acoustic aperture of either 25 λ or 111 λ, centre-frequency 100 MHz or 1000 MHz, for 128° rotated Y cut LiNbO$_3$, with SAW propagation in the X direction) in fact the intrinsic capacitance is always at least twice C_1. In the first of these design cases, the effective electrical resistance of an individual "finger" (assuming Aluminium metallisation of 0.1 μm thickness, and Si_3N_4 insulator of thickness 0.15 μm) is of the order of 6 Ω but the capacitive reactance per "finger" due to C_1 is approximately 315 Ω; in the second case, "finger" resistance is around 29 Ω and the capacitive reactance per "finger" is 730 Ω.

Application of the theory of electrical networks then leads to the following expression for the insertion loss of each such transducer:

$$\frac{\text{acoustic power out}}{\text{electrical power in}} =$$

$$\frac{2G_aR_s}{\{1 + R_sG_a - [\omega(C_1 + NC_s) + B_a]\omega L\}^2 + \{\omega LG_a + R_s[\omega(C_1 + NC_s) + B_a]\}^2} \quad (2)$$

Equations (17) and (18) of reference [4] show how to calculate G_a and B_a as functions of k^2 (the piezoelectric coupling constant) and other parameters, enabling analytic calculation of the insertion loss as a function of frequency. An example of the results
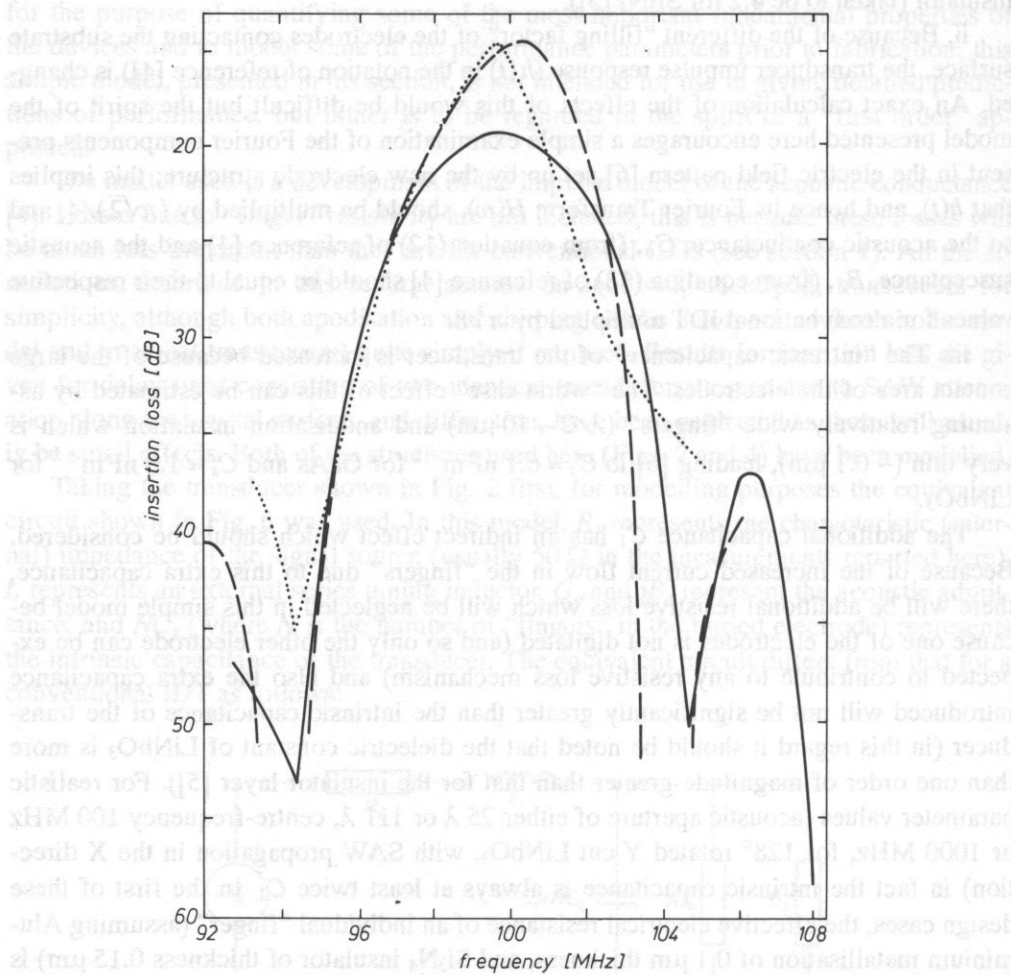

FIG. 7. Insertion loss of a delay line built using the novel transducer shown in Fig. 2: predicted (---) and experimental (···). For simplicity, no impedance-matching components were used. The material was LiNbO$_3$, the synchronous frequency was 99 MHz, transducer aperture $a = 25 \lambda$, $R_s = 50 \Omega$, $N = 20$ "fingers" and $d = 0.147 \mu m$. Also shown (—) is the frequency response of a device of the type shown in Fig. 4, using the same mask and fabricated on 128° rotated Y cut LiNbO$_3$, with SAW propagation in the X direction. Note that the symmetrical response is close to ideal.

from this expression is shown in Fig. 7, compared with some experimental results (see section 4).

Next, taking the transducer shown in Fig. 4, the equivalent circuit of Fig. 8 was used. This is identical to that used above, for the transducer shown in Fig. 2, except that a further capacitance C_1 is introduced *in series* with the acoustic admittance. This represents the capacitance between the top electrode and the substrate surface (and for a buried electrode having a 1:1 mark:space ratio, the value of this extra capacitance is equal to that introduced in parallel with the acoustic admittance in paragraph (i) above). The insertion loss per transducer, at centre-frequency, is given by

$$\frac{\text{acoustic power out}}{\text{electrical power in}} = \frac{2R_sG_a\omega^2C_1^2}{(B-AL)^2 + (D-EL)^2} \tag{3}$$

where

$$A = \omega^2G_a(2C_1 + NC_s) \tag{4}$$
$$B = G_a - \omega^2R_sC_1(C_1 + NC_s) \tag{5}$$
$$D = \omega C_1 + \omega R_sG_a(2C_1 + NC_s) \tag{6}$$
$$E = \omega^3C_1(C_1 + NC_s) \tag{7}$$

and the ideal matching inductance is given by

$$L = (AB + DE)/(A^2 + E^2). \tag{8}$$

If the insulator thickness, d, is small, the shunt capacitance is large, diverting current away from the acoustic conductance and thus reducing the acoustic power generated; if d is large, the series capacitance is small so that very little current can flow through the acoustic admittance. Therefore there is an optimal thickness of insulator at which these degrading effects are minimised collectively, giving the smallest insertion loss. Figures 9 and 10 show the centre-frequency insertion loss for delay lines fabricated on GaAs and LiNbO₃ substrates respectively, as a function of insulator thickness, for both the "tuned"(i.e. using a matching inductor with value L given by equation (8))
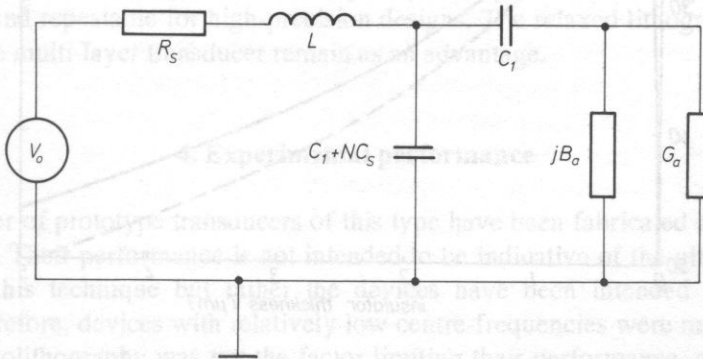

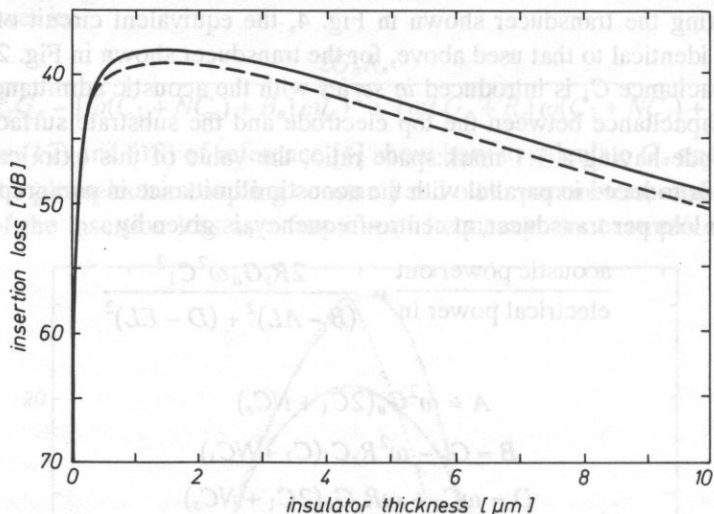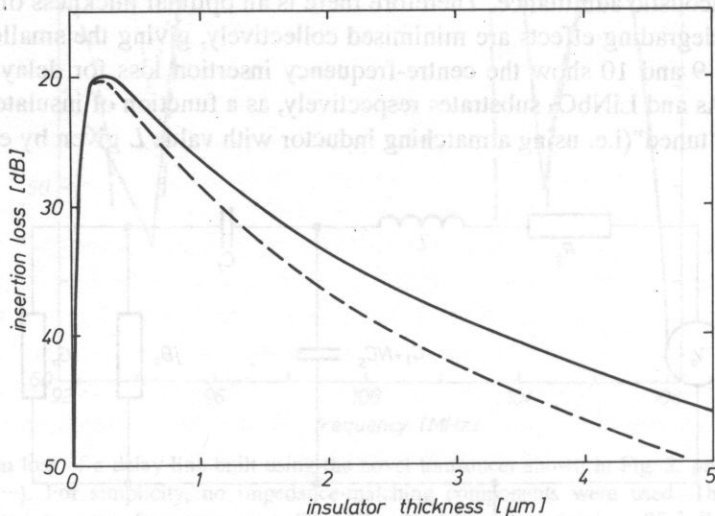FIG. 8. The equivalent circuit used in this work to model the transducer shown in Fig. 4.

FIG. 9. Predictions of insertion loss of delay lines built using the transducer shown in Fig. 4, plotted against insulator thickness, for both tuned (—) and untuned (----) cases. The substrate is {100} cut GaAs , with SAW propagation in the <011> direction, the centre frequency is 74 MHz, the transducer aperture is 25λ, the source resistance is 50 Ω, and the buried electrode consists of 20 "fingers". Optimising the value of matching inductance L makes little difference to the insertion loss.

FIG. 10. Predictions of insertion loss of delay lines built using the transducer shown in Fig. 4, plotted against insulator thickness, for both tuned (—) and untuned (----) cases. The substrate is 128° rotated Y cut LiNbO₃, with SAW propagation in the X direction, and the centre frequency is 99.7 MHz; other parameters as in Fig. 9.

and "untuned" (i.e. $L = 0$) cases. Material parameters were taken from reference [7]; the centre-frequencies for these examples were chosen to match the typical laboratory trials of the transducer which are reported in section 4. For the device parameters used the acoustic wavelength is 40 µm and the optimum insulator layer thickness is of the order of 1.5 µm for GaAs, and rather less for LiNbO$_3$. Thicknesses of this approximate magnitude are readily achievable using conventional deposition techniques and are small enough (i.e. much less than the acoustic wavelength λ) not to affect SAW propagation significantly [1]. Although at first sight it might appear that the additional capacitances introduced in the equivalent circuits for the novel transducers will significantly degrade their performance compared to conventional IDTs, this is not necessarily correct reasoning as the full network analysis shows, by taking the capacitance values into account quantitatively rather than just qualitatively. The conclusion is that the effect of the additional capacitance is not at all as disastrous as one might initially suppose.

This simple impulse-response model predicts that the performance of the two types of transducer should be similar. Direct comparison with conventional IDTs is not so straightforward but the order-of-magnitude of the insertion losses predicted for the new types of transducer is at worst comparable with that expected from conventional IDTs. (Note that when a conventional IDT is operated at the third or higher harmonic of its fundamental response, as an alternative method of obtaining operation at a higher frequency than would be normal for a given photolithographic linewidth, then its performance is correspondingly degraded). The transducers described here have an extra advantage over conventional IDTs because resistivity loss has not been taken into account in the model presented, and there is a four-fold reduction in this loss mechanism. One other effect not modelled here is that of the mechanical loading introduced by the insulator layer on top of the crystal surface. As the optimum thickness is of the order of $\lambda/20$ (or smaller) this effect will be small [1] and equivalent to that of distributed "mass loading" of the transducer, which will slightly modify the SAW velocity and hence the centre-frequency. For such a small thickness, substantial damping loss would not be expected but in any case the insertion loss may be confirmed experimentally. Similarly, the effect of the thin metal overlay electrode is anticipated to be negligible and limited to a small change in centre-frequency, unimportant in most applications but predictable and repeatable for high-precision designs. The relaxed lithography requirements for the multi-layer transducer remain as an advantage.

4. Experimental performance

A number of prototype transducers of this type have been fabricated as demonstration devices. Their performance is not intended to be indicative of the ultimate obtainable using this technique but rather the devices have been intended as feasibility studies. Therefore, devices with relatively low centre-frequencies were made so that in fact the photolithography was *not* the factor limiting their performance, and other factors could be controlled closely. Substrate crystals of LiNbO$_3$ (128° rotated Y cut)
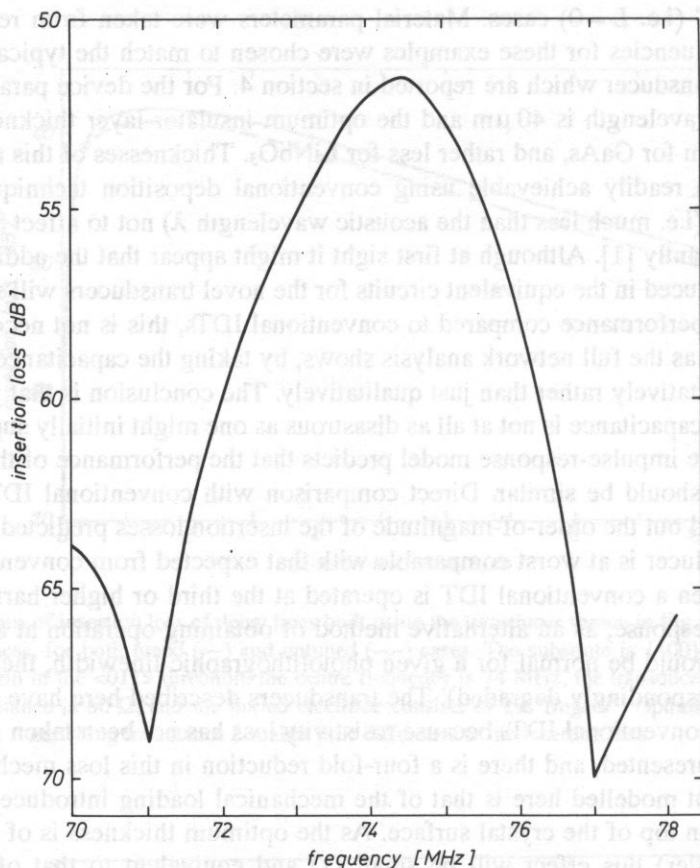
FIG. 11. The frequency response of an experimental device using unweighted transducers, of the type shown in Fig. 4, each having 20 "fingers". This device was fabricated on {100} cut GaAs, accounting for the high insertion loss; this should be compared to Fig. 7.

were used for many devices; in addition, some devices were made using GaAs ({100} cut), in order to demonstrate the fact that the fabrication method can be applied to any substrate material which can support SAW. Higher frequency devices are the subject of future work. Apodisation, in order to tailor the frequency response, has been used in order to establish the feasibility of using simple weighting techniques to produce a desired frequency response; some un-apodised devices have also been produced and tested for the purpose of establishing the fabrication procedures. Devices were tested in a 50 Ω RF system with no external matching or tuning components. Transducers fabricated as depicted in both Fig. 2 and in Fig. 4 have been fabricated and tested.

For the type shown in Fig. 2, the anodisation was omitted but the aluminium layer under the Si_3N_4 was over-etched, leading to an over-hang of the Si_3N_4 layer which was confirmed by microscopy. Then when the continuous electrode was deposited there
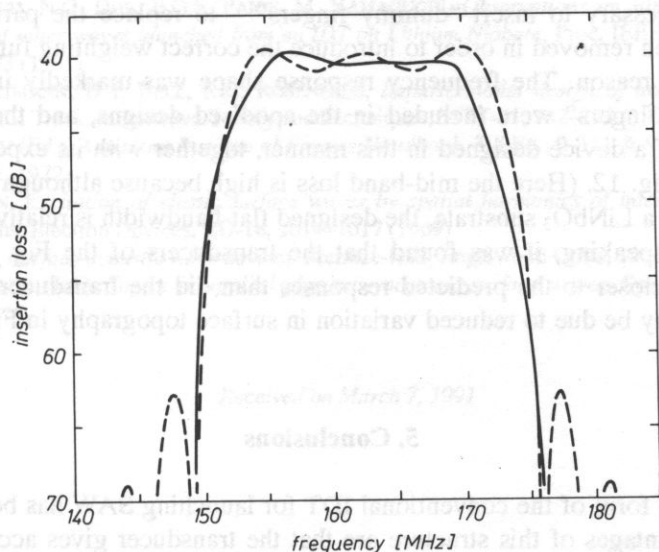
FIG. 12. The frequency response of an experimental device (——) using an apodised transducer of the type shown in Fig. 4, weighted as described in the text proportional to $\sin(2\pi t \Delta f)/t$ truncated sharply at $t = \pm 3/2\Delta f$. This device was fabricated on 128° rotated Y cut LiNbO$_3$, with SAW propagation in the X direction. Also shown is the Fourier Transform (----) of the transducer impulse response.

was an air-gap between the two electrodes so that a solid insulator along the "finger" edges was found to be unnecessary. Experimental results from this device are shown in Fig. 7.

Also shown in Fig. 7, together with Fig. 11, is the performance of a pair of devices of the type shown in Fig. 4 made on LiNbO$_3$ and GaAs substrates respectively; the transducers were all made using the same (un-apodised) mask set. The devices made using GaAs substrate material all showed a high insertion loss at centre-frequency, characteristic of a material like GaAs with a very low piezoelectric coupling constant (k^2) when used for a relatively wideband design, but the un-apodised devices using LiNbO$_3$ show much smaller insertion losses (corresponding to a much greater k^2). In this connection it should be borne in mind that the transducers used in this experimental investigation were operated without series inductors or other matching networks of any kind, and also that as all the transducers made were bidirectional the absolute minimum insertion loss was 6dB.

When apodisation is used for "finger" weighting using conventional IDTs it is normal to include "dummy fingers" across that part of the transducer aperture where the "active finger" has been removed [8]. This is done so that there is phase fidelity over the entire transducer aperture (absence of metallisation would lead to phase distortion of wavefronts travelling at the edges of the IDT aperture compared to wavefronts at the centre of the IDT aperture). Similarly, when apodising the multi-layer transducers, it

was found necessary to insert "dummy fingers" – to replace the parts of "fingers" which have been removed in order to introduce the correct weighting function – for exactly the same reason. The frequency response shape was markedly improved when such "dummy fingers" were included in the apodised designs, and the experimental performance of a device designed in this manner, together with its expected response, are shown in Fig. 12. (Here the mid-band loss is high because although this delay-line was built using a LiNbO$_3$ substrate, the designed flat-bandwidth is relatively large).

Generally speaking, it was found that the transducers of the Fig. 4 pattern performed rather closer to the predicted responses than did the transducers of the Fig. 2 pattern; this may be due to reduced variation in surface topography in Fig. 4 compared to Fig. 2.

5. Conclusions

A modified form of the conventional IDT for launching SAW has been developed. The main advantages of this structure are that the transducer gives access to SAW at higher frequencies than are possible using the conventional IDT, or alternatively a lower standard of photolithography may be used for a given device specification so that device cost is reduced. Electrical resistivity loss is less than with existing types of transducer. Some prototype devices have been fabricated and tested, and show encouraging performance. Delay-lines using apodised transducers on LiNbO$_3$ have proved the viability of apodisation as a technique for weighting the "fingers" when designing this type of transducer. It is not clear at the moment what effect lack of linewidth repeatability (at the resolution limit of photolithography) will have on the performance of these devices and so the evaluation of high frequency devices, on a statistical basis, will be a particularly valuable part of subsequent work. (It would be valuable, for example, to design a set of devices, all having the same low centre-frequency, but with the widths of the "fingers" varying in a known and controlled manner in order to simulate this effect). More complex designs such as unidirectional transducers appear to be feasible as well and will form the basis of future work.

References

[1] J.D. MAINES, E.G.S. PAIGE, *Surface-acoustic-wave components, devices and applications*, Proc. IEE, **120**, 1078–1110 (1973)
[2] K. YAMANOUCHI, T. MEGURO, K. MATSUMOTO, *Surface-acoustic-wave unidirectional transducers using anodic oxidation technology and low-loss filters*, Elect. Lett., **25**, 958–960 (1989)

[3] P.D. BLOCH, N.G. DOE, E.G.S. PAIGE, M. YAMAGUCHI, *Observations on surface skimming bulk waves and other waves launched from an IDT on Lithium Niobate*, Proc. IEEE Ultrasonics Symp., 1, 268–273 (1981)

[4] C.S. HARTMANN, D.T. BELL, R.C. ROSENFELD, *Impulse model design of acoustic surface-wave filters*, IEEE Trans. Microwave Theory and Techniques, **MTT-21**, 162–175 (1973)

[5] D.E. GRAY (Ed.), *American Institute of Physics Handbook*, 3rd Ed., 9–111 & 9–122. McGraw-Hill, New York, 1972

[6] H. ENGAN, *Excitation of elastic surface waves by spatial harmonics of interdigital transducers*, IEEE Trans. Electron Devices, **ED-16**, 1014–1017 (1969)

[7] S. DATTA, *Surface acoustic wave devices*. Prentice-Hall, Englewood Cliffs, 1986

[8] A.A. OLINER (Ed.), *Topics in applied physics – acoustic surface waves*. Springer-Verlag, Berlin, 1978